EUROPEAN FUSION DEVELOPMENT AGREEMENT

EFDA–JET–PR(04)01/25

V. Riccardo, P. Barabaschi, M. Sugihara and JET-EFDA Contributors

Characterisation of Plasma Current Quench at JET

Characterisation of Plasma Current Quench at JET

V. Riccardo, P. Barabaschi[1], M. Sugihara[2] and JET-EFDA Contributors

1 ITER International Team, Garching, Boltmannstr.2, D-85748, Germany
2 ITER International Team, Naka Joint Work Site, Naka, Ibaraki, Japan

Preprint of Paper to be submitted for publication in Plasma Physics and Controlled Fusion

ABSTRACT.
The eddy currents generated during the fastest disruption current decays represent the most severe design condition for medium and small size in-vessel components of most tokamaks. Best-fit linear and instantaneous plasma current quench rates have been extracted for a set of recent JET disruptions. Contrary to expectations, the current quench rate spectrum of high and low thermal energy disruptions is not substantially different. In addition, while disruptions are typically slower in helium plasmas than in deuterium plasmas, disruptions of low density helium plasmas following high current locked modes are actually faster than the fastest deuterium disruptions. The comparison between instantaneous and linear current decay rate shows that the linear approximation can significantly under-estimate the current decay rate in some types of disruptions. In these cases an exponential fit of the early phase of the current decay provides a more accurate estimate of the maximum current decay velocity. However, this fit is only suitable to model the fastest events, which have the current quench dominated by radiation losses rather than the plasma motion.

1. INTRODUCTION

The main direct effects of a disruption plasma current quench are the electromechanical forces that arise in the conducting structures, and in particular in the in-vessel components. The average current quench velocity is relevant for the design of large components, like the main vessel support system and the divertor attachment structure. However, the instantaneous maximum of the plasma current quench determines the design load of smaller in-vessel components. In an ITER class tokamak, these would be the modular plasma facing structures (blanket, antennas, …) and the diagnostics. In addition, the conversion of plasma current to runaway electron current due to the avalanche process is theoretically predicted to depend on the current quench rate [1].

A comprehensive set of current quench data was collected for the ITER Disruption Database (IDDB) [2]. However, a multitude of definitions was used in the various contributing machines for how to extrapolate the current decay duration. Since then it has been demonstrated [2] that the 80% to 20% interval of the pre-disruption plasma current provides the most suitable approximation of the maximum linearly-averaged plasma current decay rate. However, historically JET has always worked with the 100- 40% definition. Therefore, the basic aim of this analysis is to provide 80-20% data and to assess differences with previous approaches. Furthermore, the new JET data can be processed and compared with developments in the analysis of the same phenomenon following the IDDB work. In fact, recently detailed analysis of disruption current quenches has been carried out for JT-60U [3] and an alternative way of characterising the plasma current decay waveform is proposed for extremely fast events [4].

In section 2 the extent of the database and the procedure used for the analysis of the current quench is described. The minimum decay time normalised to the plasma area, which offers a

simple and meaningful base of extrapolation for the minimum disruption time in a new machine, is discussed in section 3. The distribution in terms of linear current quench rate is presented and discussed in section 4. The fastest events are analysed in section 5. Section 6 is dedicated to the comparison between deuterium and helium plasmas. The results are then summarised and discussed in section 7.

2. DATA SET AND ANALYSIS PROCEDURE

The database analysed here includes the disruptions of plasmas which had a plasma current higher than 1MA any time in the discharge and that occurred in JET between March 2002 and March 2004. The discharges have plasma current up to 4MA (typically between 1.5 and 3MA), toroidal field up to 4T (typically between 1.5 and 3.5T) and neutral beam power up to 22.5MW. Between March 2002 and March 2004 there has been operation with both plasma current and toroidal field reversed, with tritium as an impurity, with helium and hydrogen plasmas and neutral beams, besides normal, preparatory and high performance operation.

In the disruption database covering March 2002 to March 2004, there are 791 events, which cover the pulse range 54432 to 63445.

The plasma current signal [5] (called MG2F/XIP) has been chosen for most of the following analysis because it has never included the divertor structure current monitor, which became sporadically faulty, presenting spurious spikes at disruptions. This signal differs from more popular JET plasma current definitions also in the corrections associated with the divertor coil currents. However, the change in the divertor coil currents during the disruption is negligible with respect to the changes in the plasma current. All JET plasma current signals give an estimate of the total toroidal current within the integration domain; this includes also the toroidal component of the halo current.

For each disruption the time of the effective start of the event, t_e, is set after visual inspection. This time corresponds to the start of the plasma current increase (to counter-act the current profile flattening following the energy quench) if present or a vertical displacement faster than 10m/s. The time of the maximum plasma current, t_m, is searched after t_e and saved. Pre-disruption quantities (plasma current, area, …) are taken at t_0=t_m-0.05s. The time when the current is 100%, 80%, 40% and 20% of the pre-disruption plasma current and of the maximum plasma current are saved.

The plasma current signal is derived with respect to time, after applying a 1ms filter, between t_0 and the time when the plasma current is less than 5% of pre-disruption value. The maximum of the time derivative and the time when this occurs are saved.

3. NORMALISED QUENCH TIME

The characteristic current decay time of any disruption can be thought of as that of a coil, and so defined as the ratio between the plasma inductance and resistance. Therefore the current

quench time normalised to the pre-disruption plasma poloidal cross section is proportional to the ratio $(L_p^{eff} 2\pi R)/\eta_p$, where η_p is the plasma resistivity, *Lp eff* is the effective plasma self-inductance and R is the plasma major radius. The plasma effective inductance is $\mu_0 R$ (ln(8R/a)-2-l_i/2), with a the plasma minor radius. This typically results in $L_p^{eff/} \sim 0.60 \div 8$ $\mu_0 R$, so the area normalised disruption time is ~0.12÷0.16[(ms/m2) mΩm]/ η_p, hence inversely proportional to the plasma resistivity.

The current quench time normalised to the pre-disruption plasma poloidal cross section is plotted in Fig.1. The minimum normalised current quench times in JET are observed when the 100% to 40% interval is used to extrapolate the current decay linearly. The minimum normalised current quench time is ~2.1ms/m^2 when linearly extrapolated over the 100% to 40% of the pre-disruption plasma current. For the same event (54692, a deliberate Vertical Displacement Event, VDE) the minimum normalised current quench time is 2.66ms/m^2 over the 80% to 20% interval of the pre-disruption plasma current and 1.9ms/m^2 if extrapolated from the maximum current quench rate. While 2.66ms/m^2 is also the 80-20% minimum normalised current quench time for the database, there are events with much smaller normalised quench times extrapolated from the maximum quench rate: 41 events are in the 1.3-1.9ms/m^2 bracket. Most of these events are VDEs, which are characterised by a relatively slow current decay, with a fast phase just after the thermal quench, which typically occurs when the cylindrical approximation surface safety factor is less 1.5.

The distribution and the minimum normalised time in the 100-40% data set are consistent with those of previous JET statistical analyses [2]. In addition, taking the 80-20% definition, the minimum normalised current quench duration goes roughly as 1.25[(ms/m^2)/MA] I_{p0}. Since the typical plasma area is ~4m^2, this implies that the maximum 80-20% current quench rate is ~200MA/s, which is representative of the extreme events in the database.

4. LINEAR CURRENT QUENCH RATE

The distribution with respect to the current decay rate has been calculated using 4 definitions. These definitions differ on the interval over which the linear extrapolation is applied. They are 100-40% of the pre-disruption current (the historical JET definition), 80-20% of the pre-disruption plasma current (the preferred ITER definition), 100-40% and 80-20% of the maximum plasma current. The range of current decay rates covered has been divided into intervals 10s^{-1} wide, to ensure that in each current decay rate cell there is an adequately high number of samples. The results, plotted in Fig.2, show that there is no significant difference between the distribution obtained using the 100-40% of the pre-disruption or of the maximum plasma current or between the distribution obtained using the 80-20% of the pre-disruption or of the maximum plasma current. However, there is a significant difference between the 100- 40% and the 80-20% distributions. While both have an average of ~45s^{-1}, the standard deviation of the 100-40% distribution, 25s^{-1}, is much larger than that of the 80-20% distribution, 16s^{-1}.

The extrapolations based on 100-40% and the 80-20% intervals tend to differ the most when the decay starts slowly (e.g. as a result of MHD activity, as for pulse 58725 in Fig.3a) and only later speeds up. Neither of them gives the correct estimate of the maximum current quench rate, but the 80-20% approximation provides a better measure of the current quench duration. The way the two approaches differ in the interpretation of this set of pulses explains why the 100-40% distribution is higher at the low rate end of the spectrum in Fig.2.

At the high rate end of the spectrum, the 100-40% distribution is higher again, because of events like 55221, in Fig.3b, in which the current quench slows down towards the end (in some cases, but not always, as a result of the generation of runaway electrons). This type of event gives larger 100-40% than 80-20% current quench rates; also in this case the higher estimate is the one matching better the current decay.

In the database there are also 42 disruptions which occurred during the reverse field campaign (toroidal field and plasma current opposite to those normally used in JET). All of these happened at a pre-disruption thermal energy less than 2MJ (low for disruptions occurring during high performance, normal for disruptions following amelioration actions). These represent a very small sample and therefore any of the associated statistical analysis is subject to a large error. In Fig.4 the distribution in current quench rate of reverse field disruptions is compared with that of normal field disruptions, divided among high and low pre-disruption thermal energy. The predisruption thermal energy is defined as the diamagnetic energy measured one confinement time before the disruption time (t_e above). For simplicity, the highest reverse field thermal energy (~2MJ) has been taken as the boundary level between high and low energy for the normal field disruptions. There are 551 events at low energy and 132 at high energy among the normal field disruptions in the database, and 56 events (mainly during commissioning pulses) which do not have a reliable thermal energy measurement available. Only 12 disruptions have a thermal energy larger than 5.5MJ, with the highest in the database at ~ 8MJ. The reverse field distribution presents a peak at ~45s^{-1}, much higher than the normal field distributions and larger than any reasonable error bar. However, this peak simply results in a smaller standard deviation of 11s^{-1} for a very similar average, 42s^{-1}. The high and low pre-disruption thermal energy distributions for normal field events are very close together, suggesting that this is not a significant parameter in determining the current quench rate. This comes as a surprise since barrier collapses in ITB discharges typically occur at high thermal energy and lead to very fast current quenches. However, as it will be discussed in the following sections, these are not the only disruption types leading to high current decay rates.

5. MAXIMUM CURRENT QUENCH VELOCITY

In general, both the 80-20% and the 100-40% linear extrapolation produce an average current quench velocity which can significantly under-estimate the maximum observed, as shown in Fig.5. The maximum quench velocity can be several times the average quench velocity, nearly

independent of the averaged quench velocity. The disruptions more likely to have a very high maximum current quench velocity are events leading to the generation of runaway electrons, disruptions following low density locked modes and VDEs. Of the 21 disruptions with the highest maximum plasma current quench velocity, almost half (10) follow a barrier collapse in an ITB discharge and have various degrees of runaway conversion efficiency (up to 50% of the plasma current can be taken by the runaway electrons). The remaining events include equal numbers of VDEs following a trip of the plasma heating system, VDEs following giant ELMs, low density locked mode and density limits. In all these apart from 2 VDEs (one deliberate and one following the trip of the neutral beam heating), the current decay can be fitted better by an exponential rather than a linear function. In Table 1 the fastest 21 disruptions are listed together with their peak current decay velocity and (80-20%) average decay velocity, the inverse of the best-fit effective decay time, as suggested in [4], an estimate electron temperature, the pre-disruption plasma poloidal area and the plasma current. In all the events with a current decay that can be fitted with an exponential function, the thermal quench occurs before the start of the current decay and for all the ITB discharges at rather high values of the boundary safety factor (>3).

The exponential fitting process, and how it deals with the possible presence of a plateau along the plasma current decay due to runaway electrons, is easier to explain with reference to Fig.6. In order to minimise the effect of the runaway electron plateau, the exponential fit is based on a limited number of samples (21 samples, which cover to 4ms in total) taken in the early part of the decay. Although the sampled interval is much shorter than the duration of the whole decay, the exponential fit is able to capture the main feature of the measured plasma current in 19 of the 21 events listed in Table 1. On the other hand, the linear fit (80-20% in Fig.6) significantly underestimates the initial plasma current decay rate.

The decay rate calculated by fitting an exponential to the current decay can be used to estimate the electron temperature of the plasma. The exponent resulting from the fit is, on average, $115s^{-1}$. This is equivalent to the inverse of the R/L time of the plasma. If the plasma cross section does not vary too much in the early phases of the disruption, the plasma inductance remains nearly unchanged. Typical values for the JET plasma self-inductance are ~6μH. Therefore the typical resistance of the plasma during the disruption is ~0.7mΩ. Since the major radius is ~2.8m and the typical poloidal area is ~$4m^2$, the plasma resistivity after the thermal quench is ~0.15mΩm. The plasma temperature can be estimated to be ~3.5eV by taking the parallel resistivity, $\eta_{//}$, as half of the Spitzer's formulation for the perpendicular resistivity [6-7]:

$$\eta_{//}[\mathrm{m}\Omega] \sim 0.6510^{4}\, Z \ln \Lambda T^{-3/2}[\mathrm{K}],$$

where Z is the volume average charge of the ions, taken to be 2, and assuming ln Λ is the Coulomb logarithm (~10 for temperatures below 50eV [8]).

Reliable halo current data is available for 13 of the 21 disruptions with the highest current quench rate. In the other disruptions either the plasma moved downwards, towards the divertor, where an insufficient number of halo probes is installed to give a quantitative measure, or they occurred before the refurbished set of halo diagnostics [9] came on line. The largest product of halo fraction, f, defined as the ratio between the maximum of the toroidal average of the poloidal halo current to the pre-disruption plasma current, and toroidal peaking factor, TPF, defined as the local maximum divided by the toroidal average at the time of the maximum halo fraction, among the fast disruptions is ~0.41 for the two events with a current decay not best-fitted by an exponential. All the others have the product f·TPF less than 0.26, with the halo fraction less than 0.23. In comparison with other accidental disruptions in JET, and even more clearly with deliberate events, which have the product f·TPF respectively up to 0.47 and 0.65, these fast events do not present the most demanding halo current loads.

The halo current, and hence the electro-mechanical loads associated with it, increases as the plasma displacement at full current becomes larger [10]. In order to understand if the electro-mechanical load source due to halo and induced currents could be decoupled in JET, we need to assess whether the largest magnetic field variations are associated with the current quench rate or the plasma displacement at full current. To achieve this the maximum time derivative of the poloidal field parallel to the vessel has been collected and compared with the maximum time derivative of the plasma current. The pick-up coil chosen as representative of magnetic field changes due to the plasma displacement is located at the radial position 2.217m and at the vertical position 1.993m, that is just above the inboard edge of the upper dump plate. The significance of using this coil is that it is located where most of the upward VDEs "land" and is not protected against rapid field variations from neighbouring conductive structures (as are the coils near the divertor region). The maximum time derivative (filtered in the same way as the plasma current, with a 1ms filter) of the magnetic field divided by the predisruption plasma current is plotted versus the plasma current quench rate in Fig.7. The upper limit of the time derivative of the magnetic field is seen to be proportional to the current quench rate, while the maximum plasma displacement only depends on the vessel geometry and in VDEs weakly on the boundary safety factor. Therefore, it is reasonable to assume that the current quench, rather than the plasma displacement at full current, represents the most severe loading condition from the point of view of current induced in the conductive structures, even in this region typically severely affected by halo currents. In fact, the two events representing the upper envelope of the distribution are upwards VDEs, one accidental (58463) and one deliberate (62834).

6. DEUTERIUM AND HELIUM DISRUPTIONS

In 2001 and in 2004 a cumulative ~500 JET plasmas have been run in helium. Of these 98 disrupted. The fraction of disrupted plasmas is higher than normal, but this is justified by the unusual operating conditions, especially the difficulties in pumping helium with the cryo-pump, and

therefore in controlling the density. The disruptions of the 2001 helium campaign have been analysed in the same way as those of 2002-2004 in order to obtain data on the current quench rates. However, for all discharges the most suitable measure of the plasma current (MG2F/XIP) was not available. Consequently the maximum current quench rate cannot be discussed, as it can be affected by the spurious spikes.

The plasma current decay rate distribution is plotted along side that for low thermal energy (<2MJ, see section 4) deuterium plasmas in Fig.8. All the helium disruptions occurred when the plasma thermal energy was <2MJ. Normally helium disruptions are slower than deuterium disruptions. However, there are three disruption types that are exceptions: deliberate VDEs, radiative collapse following the end of additional heating and high current locked modes. The vertical plasma position during deliberate VDEs of helium plasmas seems to be able to displace more at constant plasma current, but when the current quench starts it has rates up to $120s^{-1}$.

Current quench rates over $160s^{-1}$ have been reached in some high current, low density disruptions due to locked modes, occurring either at the X-point formation or as soon as additional heating was applied. In particular two of these (63109 and 63111) started at 3MA and generated a loop voltage sufficient to accelerate a substantial runaway electron population. This result is not in contrast with the use of massive helium puffs to prevent the generation of runaway electrons. In fact, the background line-average electron density in the two cases is significantly different: $\sim 5\ 10^{19} m^{-2}$ for the locked mode and $\sim 20\ 10^{20} m^{-2}$ for the massive helium puff. The rationale for the runaway electron prevention by massive helium puff is supported by extensive empirical analysis of the density limit disruptions which, as shown in Fig.9, are systematically slower in helium plasmas than in deuterium plasmas, therefore providing a smaller toroidal loop voltage.

CONCLUSION

The new JET current quench database preserves the properties of the old one when the data are extracted from the interval representing the 100-40% interval of the predisruption plasma current, but presents new, and sometimes unexpected, features when different reference intervals or definitions are used. The minimum decay time normalised to the pre-disruption plasma area was and still is $\sim 2ms/m^2$ when the reference interval is 100-40%. However, exploring alternative definitions has provided evidence that the minimum quench duration depends significantly upon how it is calculated. It varies from $2.1ms/m^2$ to $2.66ms/m^2$ for the same event depending on the reference interval (either 100-40% or 80-20% of the pre-disruption plasma current). The JET poloidal area normalised quench duration is consistent with that of other machines involved in the IDDB and in more recent studies [11]. For consistently fast events the poloidal area normalised quench time is nearly the same whether estimated from the line average or the maximum time derivative. In multiphase events, the extrapolation from the maximum instantaneous time derivative can lead to a much smaller surface normalised quench time,

down to 1.3ms/m^2. In these cases, the normalised quench time can be of use to determine the inductive loads, but it is not physically related to the duration of the current quench. Also the poloidal area normalised quench duration estimated from the maximum instantaneous time derivative of the plasma current is within the scatter of recent multi-machine results (1- 2ms/m^2) [11]. Therefore if the lower limit is applied, the minimum current quench duration predicted for ITER (with a poloidal cross sectional area of ~20m^2) is about 20ms.

The maximum of the linear current decay rate is ~200MA/s, while the instantaneous maximum rate can be as large as 400MA/s. The ratio between these current decay rates strongly depends on the type of disruption. The disruptions where it is the largest are ITB collapses, VDEs and low density locked modes. In most of the fast events, the current decay is fitted better by an exponential rather than a linear function. The exponential characteristic time does not vary significantly in the set of 21 disruptions analysed and indicates that the post thermal quench electron temperature is ~3.5eV.

Analysis of the distribution of the 100-40% and the 80-20% linear approximation of the current decay rate shows that the average is kept, although the spread is different. Typical events leading to the difference between the two distributions have been identified: slow starts affect mainly the 100-40% approximation, while runaway electrons mainly the 80-20% approximation. In JET there is no significant difference in the current quench rate between high and low pre-disruption energy, while a weak dependence on the pre-disruption diamagnetic energy was instead observed in JT-60U [3]. Finally, apart from identified exceptions, disruptions of helium plasmas tend to be slower than those of deuterium plasmas. This analysis, together with similar work was carried out in JT-60U and DIII-D, expands some of the results obtained during the IDDB work to provide basic data suitable for the derivation of current quench design criteria for ITER.

ACKNOWLEDGEMENTS

This work was performed under the European Fusion Development Agreement (EFDA) and partly funded by EURATOM and the UK Engineering and Physical Sciences Research Council.

REFERANCES

[1]. M.N. Rosenbluth, S.V. Putvinski, Nuclear Fusion **37** (1997) 1355

[2]. ITER Physics Basis 1999 Nucl. Fusion **39** Chapter 3 (2332-2336)

[3]. Y. Kawano et al., Characteristics of Current Quenches of Major Disruption in JT- 60U, 30th EPS Conference on Contr. Fusion and Plasma Phys., St. Petersburg, 7-11 July 2003 ECA Vol. 27A, P-2.129

[4]. M. Sugihara et al., Examination of Plasma Behaviour during Disruptions on Existing Tokamaks and Extrapolations to ITER, 30th EPS Conference on Contr. Fusion and Plasma Phys., St. Petersburg, 7-11 July 2003 ECA Vol. 27A, P-2.139

[5]. JP Christiansen et al., Journal of Computational Physics **73** (1987) 85-106

[6]. SI Braginskii, Reviews of Plasma Physics vol I, ed M.A. Leontovich (1965, New York: Consultants Bureau) 205-287 (269)

[7]. L. Spitzer Jr, Physics of fully ionised gases, Interscience, New York, 1956, p 86

[8]. F.L. Hilton and R.D. Hazeltine, Rev. Mod. Phys. **48** (1976) 239-308 (245)

[9]. V. Riccardo et al., Fusion Engineering and Design **66-68** (2003) 919-924 15

[10]. V. Riccardo et al., Analysis of JET halo currents, accepted for publication in Plasma Physics and Controlled Fusion

[11]. M. Sugihara et al., Analysis of Disruption Scenarios and Their Mitigation in ITER, to be presented to IAEA - 20th Fusion Energy Conference, Vilamoura, Portugal 1-6 Nov 2004

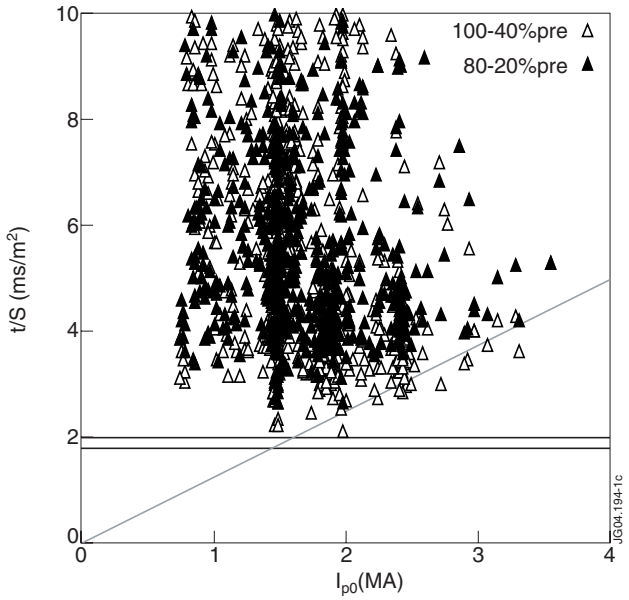

Figure.1: The current quench duration estimated from the linear extrapolation from either 100-40% or 80-20% of the pre-disruption plasma current divided by the pre-disruption poloidal cross section of the plasma is plotted versus the pre-disruption plasma current.

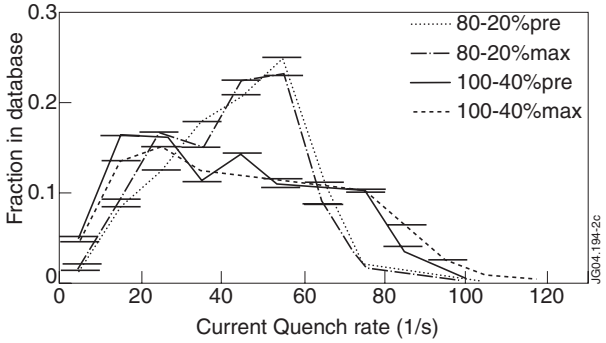

Figure.2: Distribution in plasma current quench rate of the disruptions in the database. The four definitions used for the linear extrapolation of quench rate are compared with the measured maximum quench rate.

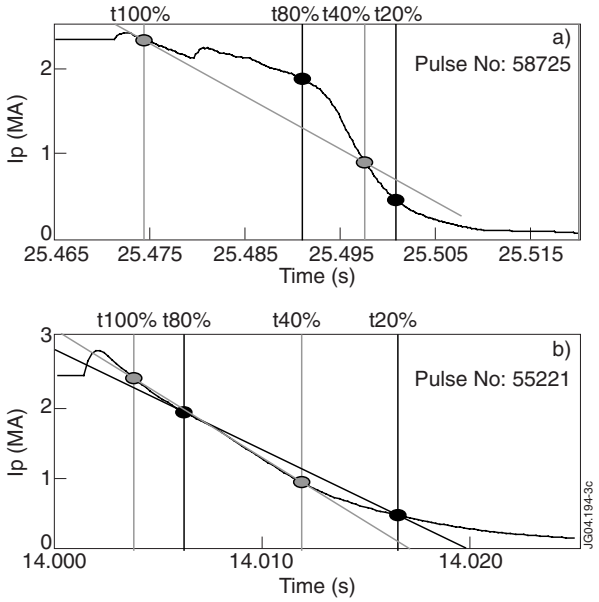

Figure.3: Typical events leading to a significant difference between the 100-40% and the 80-20% linear approximation of the current quench duration.

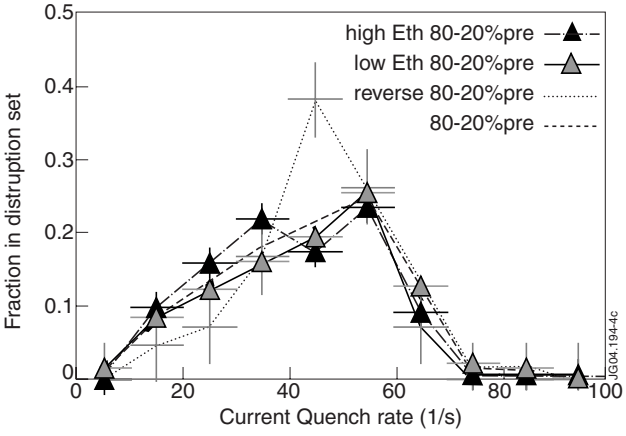

Figure.4: Current quench rate distribution for (low thermal energy) reverse field disruptions and low and high energy thermal energy normal field disruptions; the dashed line represents the overall distribution for the 80-20% definition of plasma current quench rate

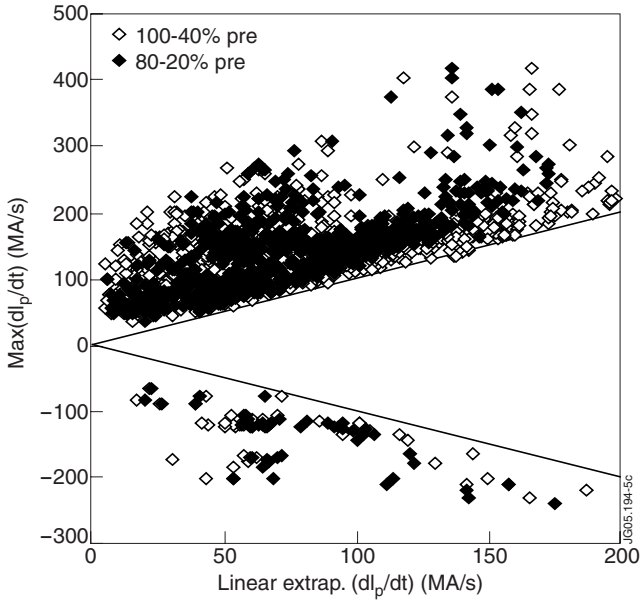

Figure.5: The maximum plasma current quench rate can be many times larger than any disruption-averaged estimate.

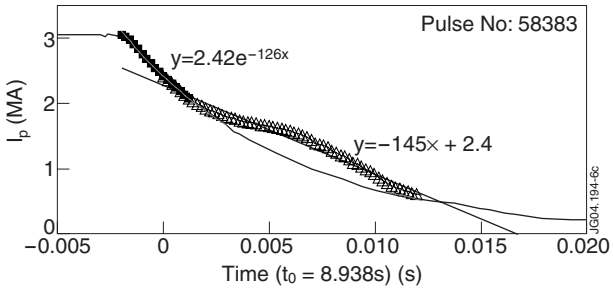

Figure.6: Linear and exponential approximation of the current decay during a disruption with very high current quench rate. The full squares are on the 21 (4ms) samples used to fit the exponential function. The open triangles are on the samples (80-20%) used to fit the current decay linearly.

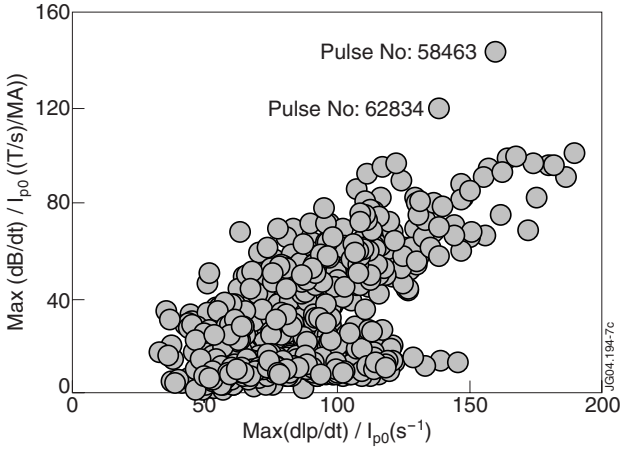

Figure.7: Maximum time derivative of the poloidal field normalised to the pre-disruption plasma current plotted versus the current quench rate.

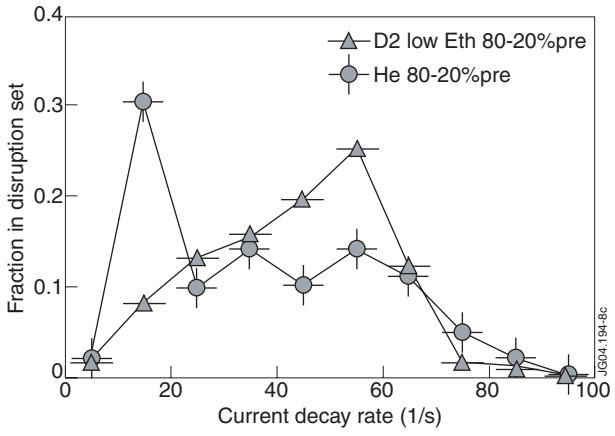

Figure.8: Current quench rate distribution for low energy deuterium and for helium disruptions

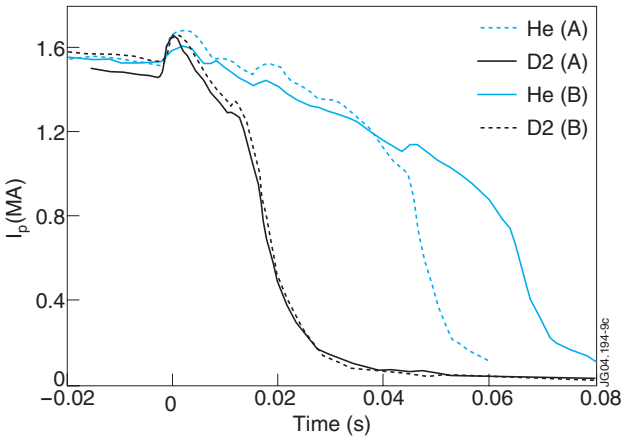

Figure.9: Plasma current following controlled density limit experiments (on the original MkII-GB): (a) Pulse No's: 53081-53998, outer divertor bleed and (b) Pulse No's: 53080-53996 inner divertor